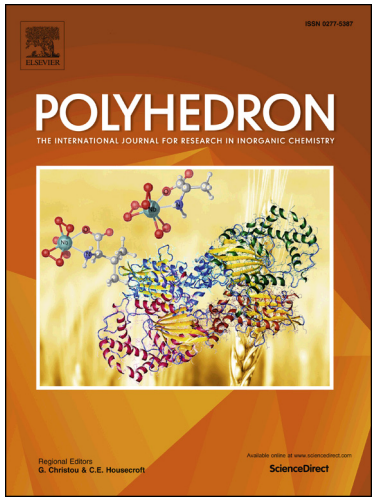

Synthesis and structural characterization of 10 Group Metal complexes with anionic tridentate *S,N,N* donor Schiff bases derived from pyridylbenzothiazolines.

Jesús-Alberto Alvarez-Hernández, Noemí Andrade-López, José G. Alvarado-Rodríguez, José M. Vásquez-Pérez, Julián Cruz-Borbolla, Vojtech Jancik

PII: S0277-5387(17)30486-2
DOI: http://dx.doi.org/10.1016/j.poly.2017.07.004
Reference: POLY 12739

To appear in: *Polyhedron*

Received Date: 7 June 2017
Revised Date: 6 July 2017
Accepted Date: 6 July 2017

Please cite this article as: J-A. Alvarez-Hernández, N. Andrade-López, J.G. Alvarado-Rodríguez, J.M. Vásquez-Pérez, J. Cruz-Borbolla, V. Jancik, Synthesis and structural characterization of 10 Group Metal complexes with anionic tridentate *S,N,N* donor Schiff bases derived from pyridylbenzothiazolines., *Polyhedron* (2017), doi: http://dx.doi.org/10.1016/j.poly.2017.07.004

Synthesis and structural characterization of 10 Group Metal complexes with anionic tridentate *S,N,N* donor Schiff bases derived from pyridylbenzothiazolines.

Jesús-Alberto Alvarez-Hernández[a], Noemí Andrade-López[a]*, José G. Alvarado-Rodríguez[a], José M. Vásquez-Pérez[b], Julián Cruz-Borbolla[a], Vojtech Jancik[c].

[a] Centro de Investigaciones Químicas, Universidad Autónoma del Estado de Hidalgo. Ciudad Universitaria, Carretera Pachuca-Tulancingo km 4.5. Colonia Carboneras, Mineral de la Reforma, Hgo. C.P. 42184, México.

[b] CONACYT Research Fellow, Universidad Autónoma del Estado de Hidalgo, Ciudad Universitaria, Carretera Pachuca-Tulancingo km 4.5. Colonia Carboneras, Mineral de la Reforma, Hgo. C.P. 42184, México.

[c] Centro Conjunto de Investigación en Química Sustentable UAEM-UNAM, km 14.5 Carr. Toluca-Atlacomulco, Unidad San Cayetano, C.P. 50200 Toluca, Edo. de México, México.

Abstract

The ring opening transformation of three substituted 2-(2-pyridyl)benzothiazolines of general formula [(C_6H_4NCS)(C_5H_4N)R] (R = C_5H_4N, **1**; R = C_6H_5, **2**; R = H, **3**) was studied by their reaction with metal chlorides of Ni(II), Pd(II), and Pt(II). In these reactions, the anionic tridentate Schiff bases {$\mathbf{L}^n$}$^-$ coordinated to metal ions were identified. Seven metallic complexes of type [M($\mathbf{L}^n$)Cl] [M = Pd, n = 1, R= C_5H_4N, (**1a**); n = 2, R = C_6H_5, (**2a**); n = 3, R = H, (**3a**). M = Pt, n = 1, R = C_5H_4N, (**1b**); n = 2, R = C_6H_5, (**2b**); n = 3, R = H, (**3b**), and M = Ni, R = C_6H_5, (**2c**)] were characterized in solution by NMR and vibrational spectroscopy in solid state. Crystal structures of benzothiazolines **1** and **2** and complexes **1a**–**3a**, **1b**·DMSO, and **2c** were analyzed by X-ray diffraction studies. In all cases, mononuclear complexes with a distorted square planar geometry were obtained. For compounds **1**–**3**, the predominance of the benzothiazoline (ring form) over the Schiff base (open form) as well as the formation of the [Pd($\mathbf{L}^n$)Cl] (n = 1–3) complexes were studied by DFT calculations at the PBEPBE/(Def2-TZVP,SDD) level in gas phase.

Keywords: Ni(II), Pd(II), Pt(II) complexes; Benzothiazolines; NMR spectroscopy; X-ray diffraction; DFT calculations.

1. Introduction

Benzothiazolines are heterocyclic compounds containing sulfur and nitrogen atoms in their structure (Figure 1, left), and have been utilized for the transference of hydrogen for the reduction of imines [[1], [2]], as well as for the synthesis of benzothiazoles and benzothiazines used as ligands in Coordination Chemistry [[3], [4]]. Interestingly, the benzothiazolines can be transformed into their open form (Figure 1) by means of a tautomerization as has been observed by NMR studies in solution; this open form is enhanced by the formation of intramolecular hydrogen bonding, while the lacking of such interactions has an opposite effect [[5], [6], [7]]. Additionally, the metallic complexation of benzothiazoline compounds has been employed to evaluate this opening along with the coordination of their corresponding Schiff bases (Figure 1 right), which are not possible to synthesize by condensation reactions of aldehydes or ketones with *o*-aminothiophenol [[8], [9]]. In these studies, the metallic ion has been used as a template reagent, and κ^2*N*κ*S*-, κ^3*N*- and κ*N*κ^2*S*-tridentate coordination modes of the Schiff bases to the central atom have been observed [[10], [11], [12]]. It is noteworthy that the nature of the substituents joined to the carbon flanked by the sulfur and nitrogen atoms has a relevant influence onto the observed isomer (ring vs. open form) [[13], [14]].

Herein we describe the reactivity of 2-pyridylbenzothiazolines with different R groups towards metal dichlorides of the 10 Group to study the effect of the distinct substituents such as pyridine, phenyl, or hydrogen attached to the carbon present in the heterocyclic thiazoline ring. The benzothiazoline compounds were transformed into their corresponding Schiff bases upon metal coordination, yielding metallic complexes of general formula [M(**L**^{n})Cl] (M = Ni, Pd, Pt; n = 1–3). The benzothiazoline precursors **1**–**3** as well as the Ni(II), Pd(II), and Pt(II) complexes were structurally characterized by vibrational spectroscopy, ^{1}H and ^{13}C NMR, and by single crystal X-Ray diffractions studies. The tautomeric equilibria of **1**–**3** precursors and the formation of the Pd(II) complexes were explored by DFT approaches.

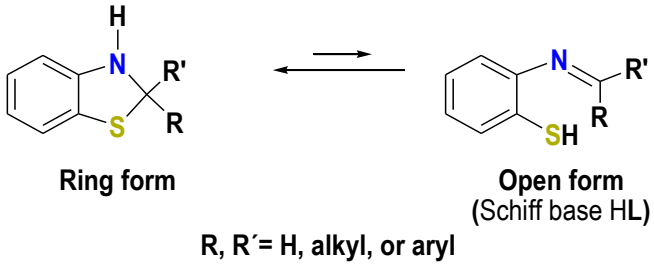

Figure 1. Structure of benzothiazolines and their corresponding H**L** Schiff base isomers.

2. Experimental

2.1 General details

All the manipulations of air and moisture sensitive materials were carried out under dinitrogen atmosphere using Schlenk techniques. Solvents such as acetonitrile (MeCN) and dimethylsulfoxide (DMSO) were dried according to the standard methods and distilled before their use. $PdCl_2$, $PtCl_2$, and $NiCl_2{\cdot}6H_2O$ were purchased from Aldrich and used as received. The $[M(NCMe)_2Cl_2]$ complexes (M = Pd, Pt) used as starting materials were prepared and isolated as reported [[15]]. Melting points were recorded on a Mel-Temp II apparatus and are reported without correction. Elemental analyses were performed on a Perkin–Elmer Series II CHNS/O Analyzer 2400. Infrared spectra were recorded on a FT-IR 200 Perkin–Elmer spectrophotometer in the 4000–400 cm^{-1} range using KBr pellets, CsCl, or $CHCl_3$. NMR spectra were obtained on a Varian NMRS 400 spectrometer in DMSO-d6 solutions at 399.78 MHz for ^1H and 100.53 MHz for $^{13}C\{^1H\}$ spectra. Chemicals shifts (ppm) of ^1H and $^{13}C\{^1H\}$ spectra are relative to the frequency of $SiMe_4$. NMR assignments of compounds **1** and **2** and complexes $[M(\mathbf{L}^n)Cl]$ [n = 1–3; M = Pd (**1a**–**3a**); Pt (**1b**–**3b**) were performed by two-dimensional heteronuclear and mononuclear experiments (COSY, HSQC, and HMBC).

Single crystals of **1** and **2** were grown by slow evaporation of a diethylether solution at room temperature. Crystals of **1a**, **2a**, **3a**, and **2c** were crystallized at room temperature by slow evaporation from an acetonitrile and toluene 1:1 mixture. Crystals of **1b** were grown as DMSO solvate from a supersaturated

solution of a dimethylsulfoxide solution. Intensity data were collected at 295 K on a Gemini CCD diffractometer with either graphite-monochromated Mo-Kα radiation (λ = 0.71073 Å) for **1**, **2**, **2a**, **1b**·DMSO, **2c**, and **3a** or Cu-Kα radiation (λ = 1.54184 Å) for **1a**. Data were integrated, scaled, sorted, and averaged using the CrysAlis software package [[16]].

The initial structures were solved by using intrinsic phasing (SHELXT) and refined with the ShelXTL [[17]] refinement package with the Olex2 suite [[18]] by using least squares minimization against F^2. Anisotropic displacement parameters for non-H atoms were refined; the positions of the hydrogen atoms were kept fixed with a common isotropic displacement parameter at 1.2 times of all C(H) groups. The crystal data and structure refinement details for compounds **1**, **2**, **1a**–**3a**, **1b**·DMSO, and **2c** are collected in Table 1.

For the DFT studies, atomic coordinates of benzothiazolines **1**–**3** and complexes **1a–3a** were obtained from X-ray crystallography while coordinates of acetonitrile and [$PdCl_2$] were obtained from the NIST [[19]] and COD databases [[20]]. Multiple reaction pathways were proposed based on molecular dynamics simulations of compounds **1**–**3** calculated with the DFTB+ software [[21]], and from the known coordination modes of palladium(II) cation. Molecular structures of stable intermediates; i.e., minima on the potential energy surface, were optimized and used as starting points to locate the corresponding transition states by either the double end interpolation method or scanning of reaction coordinates. Then, intrinsic reaction coordinate (IRC) calculations were performed to ensure that every minimum was actually connected by one transition state. All optimizations and coordinate scans were performed with the Gaussian 09 software [[22]] at the SVWN/SVP,SDD level of theory in gas phase, while saddle interpolations were performed with de deMon2k software [[23]] at the SVWN/DZVP level of theory. For the calculation of the Gibbs free energy profiles, all intermediates were recalculated at the PBEPBE/(Def2-TZVP,SDD) level of theory in gas phase at 273 K, performing normal mode analysis and verifying that all minima and transition states had zero and one imaginary frequencies, respectively. Activation barriers $\Delta G^{\dagger}$ for each mechanism were calculated as the energy difference between the

first step in the reaction path and the highest point along it, while free energy changes ΔG were calculated as the energy difference between first and last steps on the reaction path.

2.2 Synthesis of benzothiazolines 1–3

The compounds **1–3** were obtained from the reaction of *o*-aminothiophenol with the corresponding aldehyde or ketone derivative, Scheme 1.

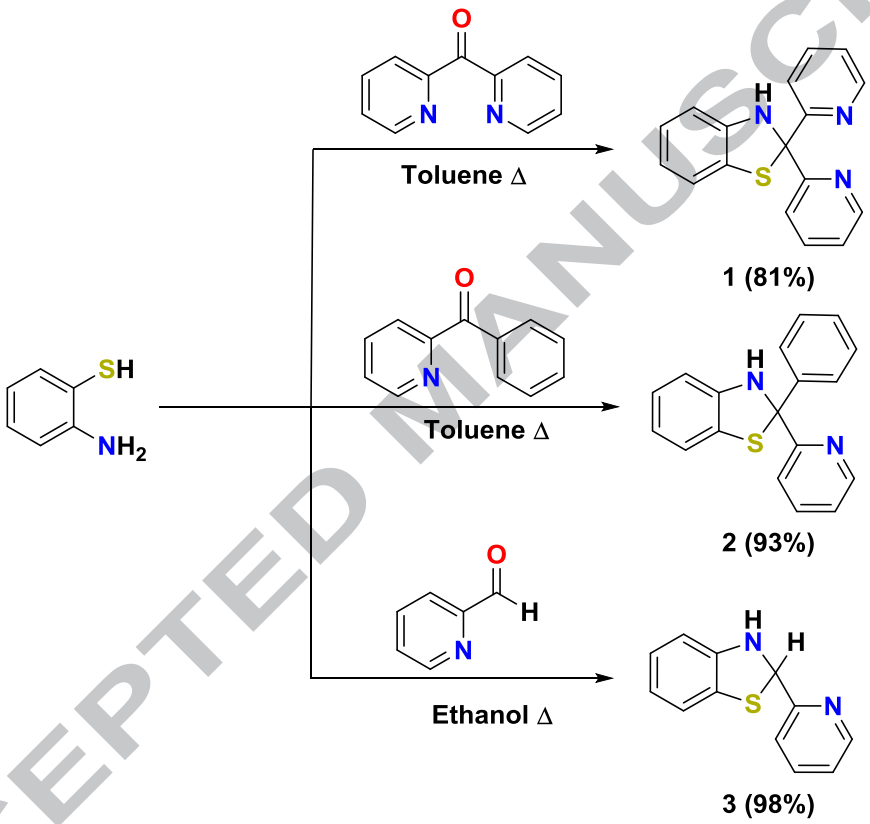

Scheme 1. Synthesis of benzothiazolines **1–3**.

A mixture of the substituted 2-(pyridyl)ketone [$C_5H_4NC(O)R$; R = C_5H_4N, C_6H_5] with *o*-aminothiophenol in a 1:1.2 ratio, catalytic amounts of sulfuric acid (three drops), and 0.50 g of sodium sulfate anhydrous in 50 mL of toluene was refluxed for 12 h (**1**) or 72 h (**2**). Then, the mixture was cooled to room temperature and the sodium sulfate was filtered off. The solution was evaporated to dryness and a yellow oil

was obtained; it was dissolved in 25 mL of dichloromethane and extracted with water (5 × 5 mL). The organic phase was dried with sodium sulfate anhydrous, filtered, and evaporated to give yellow solids that were identified as compounds **1** and **2**. Compound **3** was synthesized as previously has been reported. [**Error! Bookmark not defined.**]

*2.2.1 Compound **1***

Di(2-pyridyl)ketone (1.00 g, 5.42 mmol), *o*-aminothiophenol (1.02 g, 8.13 mmol) Yellow solid. Yield: 81% (1.27 g). M. p.: 140–142°C. Anal. Calc. for $C_{17}H_{13}N_3S$ (%): C, 70.08; H, 4.50; N 14.42. Found: C, 70.43; H, 4.14; N, 14.62. IR data (CsCl, cm^{-1}): 3287 (NH), 1571 (C=N). ^{1}H NMR (DMSO-d6) δ = 8.46 (dd, H5, 2H, ^{3}J = 4.80, ^{4}J = 1.60 Hz), 7.88 (d, H2, 2H, ^{3}J = 8.00 Hz), 7.84 (s, broad, NH, 1H), 7.82 (ddd, H3, 2H, ^{3}J = 8.00, ^{3}J = 8.00, ^{4}J = 1.60 Hz), 7.25 (ddd, H4, 2H, ^{3}J = 7.20, ^{3}J = 4.60, ^{4}J = 1.60 Hz), 7.02 (d, H12, 1H, ^{3}J = 7.20 Hz), 6.87 (ddd, H10, 1H, ^{3}J = 7.60, ^{3}J = 7.60, ^{4}J = 1.60 Hz), 6.80 (dd, H9, 1H, ^{3}J = 8.00, ^{4}J = 1.00 Hz), 6.59 (ddd, H11, 1H, ^{3}J = 7.60, ^{3}J = 7.20, ^{4}J = 1.20 Hz). ^{13}C{^{1}H} NMR (DMSO-d6) δ = 163.0 (C1), 148.6 (C5), 146.9 (C8), 136.9 (C3), 125.5 (C10), 124.0 (C7), 122.5 (C4), 121.0(C12), 120.8 (C2), 118.9 (C11), 109.6 (C9), 85.3 (C6).

*2.2.2 Compound **2***

2-benzoylpyridine (1.00 g, 5.46 mmol), *o*-aminothiophenol (1.023 g, 8.19 mmol). Yellow solid. Yield: 93% (1.47 g). M. p.: 115–117°C. Anal. Calc. for $C_{18}H_{14}N_2S$ (%): C, 74.45; H, 4.86; N, 9.65. Found: C, 74.42; H, 4.99; N 9.89. IR data (CsCl, cm^{-1}): 3295 (NH), 1570 (C=N). ^{1}H NMR (DMSO-d6) δ = 8.55 (d, 1H, H5, ^{3}J = 4.80 Hz), 7.86 (ddd, 1H, H3, ^{3}J = 7.83, ^{3}J = 7.83, ^{4}J =1.75 Hz), 7.83 (s, broad, 1H, NH), 7.78 (dd, 1H, H2, ^{3}J = 8.00, ^{4}J = 0.80 Hz), 7.53 (d, 2H, H14, H18, ^{3}J = 8.33 Hz), 7.31 (m, 3H, H4, H15, H17), 7.22 (dd, 1H, H16, ^{3}J = 7.59, ^{3}J = 7.19 Hz), 7.02 (d, 1H, H12, ^{3}J = 7.44 Hz), 6.90 (ddd,1H, H10, ^{3}J = 7.59, ^{3}J = 7.59, ^{4}J =1.20 Hz), 6.77 (d, 1H, H9, ^{3}J =7.83 Hz), 6.60 (ddd, 1H, H11, ^{3}J = 7.59, ^{3}J = 7.59, ^{4}J = 1.20 Hz). ^{13}C{^{1}H} NMR (DMSO-d6) δ = 163.8 (C1), 149.4 (C5), 147.1 (C8), 146.1 (C13), 137.6 (C3),

128.5 (C15, C17), 127.8 (C16), 126.7 (C14, C18), 125.9 (C10), 124.8 (C7), 122.9 (C4), 121.5 (C12), 120.4 (C2), 119.3 (C11), 109.5 (C9), 85.1 (C6).

*2.2.3 Compound **3***

2-pyridinecarboxaldehyde (0.30 g, 2.80 mmol), *o*-aminothiophenol (0.35 g, 2.80 mmol). Yellow solid. Yield: 98% (0.592 g). M. p.: 93–95°C. IR data (CsCl, cm^{-1}): 3392, 3230 (NH), 1571 (C=N). ^{1}H NMR (DMSO-d6) δ = 8.52 (dd, H5, 1H, ^{3}J = 4.80, ^{3}J = 2.00 Hz), 7.81 (ddd, H3,1H, ^{3}J = 7.80, ^{3}J = 7.60, ^{4}J = 2.00 Hz), 7.56 (d, H2, 1H, ^{3}J = 8.00 Hz), 7.32 (ddd, H4,1H, ^{3}J = 7.60, ^{3}J = 5.00, ^{4}J = 1.20 Hz), 7.12 (d, 1H, NH, ^{3}J = 2.80 Hz), 7.00 (d. H12, 1H, ^{3}J = 7.60 Hz), 6.92 (ddd, H10, 1H, ^{3}J = 7.60, ^{3}J = 7.60, ^{4}J = 1.20 Hz), 6.67(dd, 1H, H9, ^{3}J = 7.80, ^{4}J = 1.20 Hz), 6.61 (ddd, H11, 1H, J^{3} = 7.60, ^{3} J = 7.20, ^{4}J = 1.20 Hz), 6.40 NH (d, H6, 1H, ^{3}J = 2.80 Hz). $^{13}C\{^{1}H\}$ NMR (DMSO-d6) δ = 161.8 (C1), 149.0 (C5), 147.8 (C8), 137.3 (C3), 125.4 (C10), 124.5 (C7), 123.0 (C4), 121.2 (C12), 119.8 (C2), 118.9 (C11), 108.9 (C9), 69.6 (C6).

2.3 Synthesis of metallic complexes

*2.3.1 Synthesis of bidentate complex [Pd(**1**)Cl_2]*

An equimolar mixture of [Pd($NCCH_3$)$_2Cl_2$] (0.080g, 0.37 mmol) in 25 mL of acetonitrile with **1** (0.107 g, 0.37 mmol) was stirred at 0°C for 24 h. Then, the obtained yellow solid was filtered off and dried in vacuum. The solid formed was washed with cold acetonitrile (10 mL) and was filtered off and dried by suction. Yield: 89% (0.090 g). Dec.: 212°C. Anal. Calc. for [Pd($C_{17}H_{12}N_3S$)Cl_2] (%): C, 43.66; H, 2.59; N, 8.98. Found: C, 43.94; H, 2.75; N, 8.42. IR data (KBr, cm^{-1}): 3231 (NH), 1600 (C=N), 1580, 1471 (C=C). ^{1}H NMR (DMSO-d6) δ = 9.00 (dd, 1H, H5, ^{3}J = 5.69, ^{4}J = 1.20 Hz), 8.82 (s, 1H, NH), 8.19 (ddd, 2H, H3, ^{3}J = 8.20, ^{3}J = 7.40, ^{4}J = 1.20 Hz), 7.94 (d, 2H, H2, ^{3}J = 7.60 Hz), 7.58 (ddd, 2H, H4, ^{3}J = 6.80, ^{3}J = 6.60, ^{4}J = 1.20 Hz), 7.17 (d, 1H, H12, ^{3}J = 7.60 Hz), 7.06 (ddd, 1H, H10, ^{3}J = 8.00, ^{3}J =7.20, ^{4}J = 1.20 Hz), 7.02 (d, 1H, H9, ^{3}J = 8.00 Hz), 6.72 (ddd, 1H, H11, ^{3}J

= 7.60, ^{3}J =7.20, ^{4}J = 1.20 Hz). $^{13}C\{^{1}H\}$ NMR (DMSO-d6) δ = 156.3 (C5), 154.5 (C1), 144.9 (C8), 141.4 (C3), 126.7 (C10), 125.5 (C4), 122.5 (C2), 122.2 (C7), 121.8 (C12), 119.9 (C11), 109.5 (C9), 83.8 (C6).

2.4 Synthesis of complexes [M(L^{1})Cl] (M = Pd, Pt).

General Procedure

An equimolar mixture of $[M(NCCH_3)_2Cl_2]$ (M = Pd, Pt) with the benzothiazoline **1** in 25 mL of acetonitrile was refluxed (M= Pd, 2 h; M = Pt, 18 h). The green solid obtained was filtered off and dried in vacuum. Then, this solid was identified by NMR as the mixture of complexes [Pd(**1**)Cl_2] and [Pd(**L^{n}**)Cl] in a 20:80 ratio in the case of M = Pd, while in the case M = Pt the mixture was observed in a 50:50 ratio of [Pt(**L^{1}**)Cl] and an unidentified compound. Each mixture was suspended in 5 mL of dimethylsulfoxide and heated until dissolution at 60 °C (M = Pd) and 80°C (M = Pt) for 10 minutes. Afterward, the reaction mixture was cooling to room temperature, the brown solid formed was filtered off and dried in vacuum.

*2.4.1 [Pd(**L^{1}**)Cl] (**1a**)*

$[Pd(NCCH_3)_2)Cl_2]$ (0.122 g, 0.26 mmol). Green solid. Yield: 98% (0.11 g). M. p.: 300 ^{o}C. Anal. Calc. for $[Pd(C_{17}H_{12}N_3S)Cl]\cdot(CH_3)_2SO$ (%): C, 44.71; H, 3.55; N, 8.23. Found (%): C, 44.64; H, 3.58; N, 7.95. IR data (KBr, cm^{-1}): 1594, 1534 (C=N); 1580, 1461 (C=C). ^{1}H NMR (DMSO-d6) δ = 8.89 (d, 1H, H5, ^{3}J = 4.80 Hz), 8.70 (d, 1H, H17, ^{3}J = 5.20 Hz), 8.14 (ddd, 1H, H3, ^{3}J = 8.00, ^{3}J = 7.60, ^{4}J = 1.60 Hz), 8.06 (ddd, 1H, H15, ^{3}J = 7.80, ^{3}J = 7.60, ^{4}J =1.60 Hz), 7.89 (d, 1H, H2, ^{3}J = 8.00 Hz), 7.76 (m, 2H, H4, H16), 7.07 (d, 1H, H14, ^{3}J = 7.60 Hz), 7.02 (d, 1H, H12, ^{3}J = 7.60 Hz), 6.89 (ddd, 1H, H11, ^{3}J = 7.60, ^{3}J = 7.20, ^{4}J = 1.20 Hz), 6.38 (ddd, H10, 1H, ^{3}J = 8.00, ^{3}J = 7.60, ^{4}J =1.20 Hz), 5.63 (d, 1H, H9, ^{3}J = 8.80 Hz). $^{13}C\{^{1}H\}$ NMR (DMSO-d6) δ = 165.9(q, C6), 159.6 (q, C13), 155.4 (q, C7), 151.3 (C5), 150.5 (q, C1), 148.5 (C17), 143.5(q, C8), 140.9 (C15), 138.7 (C3), 130.9 (C11), 130.0 (C12), 129.5 (C14), 128.8 (C16), 126.1 (C4), 124.2 (C2), 123.3 (C9), 121.8 (C10).

*2.4.2 [Pt(**L**^{1})Cl] (**1b**)*

[Pt(NCCH$_3$)$_2$)Cl$_2$] (0.080 g, 0.230 mmol), **1** (0.067 g, 0.230 mmol). Green solid. Yield: 42% (0.05 g). M. p.: 245–250 °C. Anal. Calc. for [Pt(C$_{17}$H$_{12}$N$_3$S)Cl] (%): C, 39.20; H, 2.32; N, 8.07. Found (%): C, 38.93; H, 2.28; N, 7.14. IR data (KBr, cm^{-1}): 1595, 1520 (C=N); 1582, 1459 (C=C). ^{1}H NMR (DMSO-d6) δ = 8.91 (m, 2H, H5, H17), 8.17 (ddd, 1H, H3, ^{3}J = 7.60, ^{3}J = 5.20, ^{4}J = 1.60 Hz), 8.07 (ddd, 1H, H15, ^{3}J = 8.00, ^{3}J = 7.80, ^{4}J = 1.60 Hz), 7.93 (dd, 1H, H2, ^{3}J = 7.60, ^{4}J = 1.20 Hz), 7.82 (ddd, 1H, H16, ^{3}J = 7.80, ^{3}J = 5.20, ^{4}J = 1.20 Hz), 7.75 (ddd, 1H, H4, ^{3}J = 6.60, ^{3}J = 5.20, ^{4}J = 1.20 Hz), 7.07 (dd, 1H, H12, ^{3}J = 8.00, ^{3}J = 1.20 Hz), 6.93 (d, 1H, H14, ^{3}J = 8.00 Hz), 6.82 (ddd, 1H, H11, ^{3}J = 8.00, ^{3}J = 7.20, ^{4}J = 1.20 Hz), 6.30 (ddd, 1H, H10, ^{3}J = 8.80, ^{3}J = 7.20, ^{4}J = 1.20 Hz), 5.54 (d, 1H, H9, ^{3}J = 8.80 Hz). ^{13}C{^{1}H} NMR (DMSO-d6) δ = 171.0 (q, C6), 160.9 (q, C13), 156.5 (q, C7), 151.6 (C5), 150.2 (q, C1), 146.8 (C17), 145.1 (q, C8), 140.8 (C15), 138.9 (C3), 132.2 (C11), 131.2 (C14), 130.9 (C16), 130.6 (C12), 126.4 (C4), 124.7 (C2), 124.3 (C9), 121.4 (C10).

2.5 Synthesis of complexes [M(L^n)Cl] (n = 2, 3; M = Pd, Pt).

General Procedure

An equimolar mixture of [M(NCCH$_3$)$_2$Cl$_2$] (M = Pd, Pt) with the corresponding benzothiazoline (**2** or **3**) in 25 mL of acetonitrile was refluxed (M= Pd, 2 h; M = Pt, 5 h). After cooling to room temperature, the mixture reaction obtained was filtered off and dried in vacuum to give a stable solid at room temperature. The solid obtained by filtration and by evaporation of the organic phase was identified as the corresponding complex of formula [M(**L**^{n})Cl] (M = Pd, Pt; n = 2, 3).

*2.5.1 [Pd(**L**^{2})Cl] (**2a**)*

[Pd(NCCH$_3$)$_2$Cl$_2$] (0.080 g, 0.310 mmol), ***2*** (0.090 g, 0.310 mmol). Brown solid. Yield: 88% (0.118 g). M. p.: 300 ^{o}C. Anal. Calc. for [Pd(C$_{18}$H$_{13}$N$_2$S)Cl]·0.5H$_2$O (%): C, 49.11; H, 3.21; N, 6.36. Found (%): C, 49.37; H, 3.04; N, 5.52. IR data (KBr,

cm^{-1}): 1592, 1575 (C=N); 1592, 1469 (C=C). ^{1}H NMR (DMSO-d6) δ = 8.69 (d, 1H, H5, ^{3}J = 5.17 Hz), 8.07 (t, 1H, H3, ^{3}J = 7.89 Hz), 7.76 (dd, 1H, H4, ^{3}J = 5.99, ^{3}J = 6.80 Hz), 7.71 (m 3H, H15, H16, H17), 7.65 (m, 2H, H14, H18), 7.03 (d, 1H, H2, ^{3}J = 7.97 Hz), 7.00 (d, 1H, H12, ^{3}J = 7.59 Hz), 6.88 (t, 1H, H11, ^{3}J = 7.39 Hz), 6.36 (t, 1H, H10, ^{3}J = 7.78 Hz), 5.95 (d, 1H, H9, ^{3}J = 8.68 Hz). $^{13}C\{^{1}H\}$ NMR (DMSO-d6) δ = 169.0 (q, C6), 160.9 (C1), 155.0 (C7), 148.1 (C5), 144.4 (C8), 141.0 (C3) 133.2 (C13), 131.3 (C16), 130.8 (C11), 130.5 (C15, 17), 130.2 (C12), 129.8 (C2), 128.8 (C4), 127.6 (C14, 18), 124.1 (C9), 121.7 (C10).

*2.5.2 [Pt(**L**^{2})Cl] (**2b**)*

[$Pt(NCCH_3)_2Cl_2$], (0.080 g, 0.230 mmol), **2** (0.066 g, 0.230 mmol). Green solid. Yield: 56% (0.068 g). M. p.: 305-310°C. Anal. Calc. for [$Pt(C_{18}H_{13}N_2S)Cl$]: C, 41.58; H, 2.52; N, 5.39. Found (%): C, 40.96; H, 2.47; N, 4.35.R data (KBr, cm^{-1}): 1596, 1577 (C=N); 1596, 1471 (C=C). ^{1}H NMR (DMSO-d6) δ = 8.91 (d, 1H, H5, ^{3}J = 5.40 Hz), 8.06 (ddd, 1H, H3, ^{3}J = 7.60, ^{3}J = 7.20, ^{4}J = 1.60 Hz), 7.77 (ddd, 1H, H4, ^{3}J = 7.20, ^{3}J = 5.40, ^{4}J = 1.20 Hz), 7.71 (m, 3H, H15, H16, H17), 7.64 (m, 2H, H14, H18), 7.04 (d, 1H, H12, ^{3}J = 9.20 Hz), 6.87 (d, 1H, H2, ^{3}J = 7.60 Hz), 6.80 (ddd, 1H, H11, ^{3}J = 9.20, ^{3}J = 7.60, ^{4}J = 1.20 Hz), 6.26 (ddd, 1H, H10, ^{3}J = 8.80, ^{3}J = 7.60, ^{4}J = 1.60 Hz), 5.94 (d, 1H, H9, ^{3}J = 8.80 Hz). $^{13}C\{^{1}H\}$ NMR (DMSO-d6) δ = 173.9 (C6), 161.7 (C1), 156.2 (C7), 146.4 (C5), 145.6 (C8), 140.6 (C3), 132.6 (C13), 131.7 (C11), 131.3 (C2), 131.2 (C12), 130.5 (C4,C16), 130.4 (C15, C17), 127.8 (C14, C18), 124.7 (C9), 121.2 (C10).

*2.5.3 [Pd(**L**^{3})Cl] (**3a**)*

[$Pd(NCCH_3)_2Cl_2$] (0.080 g, 0.310 mmol), **3** (0.066 g, 0.310 mmol). Orange solid. Yield: 82% (0.091 g). M. p.: 318 ^{o}C. Anal. Calc. for [$Pd(C_{12}H_9N_2S)Cl$] (%): C, 32.48; H, 2.04; N, 6.31. Found (%): C, 32.32; H, 2.00; N, 5.55. IR data (KBr, cm^{-1}): 1601, 1570 (C=N); 1583, 1475 (C=C). ^{1}H NMR (DMSO-d6) δ = 9.00 (s, 1H, H6), 8.55 (dd, 1H, H5, ^{3}J = 5.40, ^{4}J = 1.60 Hz), 8.22 (ddd, 1H, H3, ^{3}J = 7.60, ^{3}J = 7.80, ^{4}J = 1.60 Hz), 7.95 (d, 1H, H2, ^{3}J = 8.00 Hz), 7.78 (ddd, 1H, H4, ^{3}J = 8.00, ^{3}J =

5.20, ^{4}J = 1.20 Hz), 7.55 (d, 1H, H9, ^{3}J = 8.40 Hz), 7.07 (m, 2H, H12, H11), 6.93 (ddd, 1H, H10, ^{3}J = 7.60, ^{3}J = 7.40, ^{4}J = 1.60 Hz). $^{13}C\{^{1}H\}$ NMR (DMSO-d6) δ =158.9 (C6),158.3 (C1),152.2 (C7), 148.6 (C5), 143.8 (C8), 141.2 (C3), 131.7 (C11), 129.4 (C12), 129.0 (C2), 128.8 (C4), 122.8 (C10), 118.8 (C9).

*2.5.4 [Pt(**L**^{3})Cl] (**3b**)*

[$Pt(NCCH_3)_2Cl_2$] (0.080 g, 0.230 mmol), **3** (0.049 g, 0.230 mmol). The brown solid obtained by filtration and dried in vacuum. Yield: 60 % (0.061 g). M. p.: above 330 ^{o}C. Anal. Calc. for [$Pt(C_{12}H_9N_2S)Cl$] (%): C, 32.48; H, 2.04; N, 6.31. Found (%): C, 32.32; H, 2.00; N,5.55. IR data (KBr, cm^{-1}): 1605, 1568 (C=N); 1580, 1473 (C=C). ^{1}H NMR (DMSO-d6) δ = 9.20 (s, 1H, H6, $^{3}J_{1H\text{-}195Pt}$ = 46.77 Hz), 8.75 (dd, 1H, H5, ^{3}J = 5.20, ^{4}J = 1.00 Hz), 8.21 (ddd, 1H, H3, ^{3}J = 8.00, ^{3}J = 7.60, ^{4}J = 1.60 Hz), 7.81 (m, 2H, H2, H4), 7.51 (d, 1H, H9, ^{3}J = 7.60 Hz), 7.12 (dd, 1H, H12, ^{3}J = 8.40, ^{4}J = 1.20 Hz), 7.02 (ddd, 1H, H11, ^{3}J = 8.40, ^{3}J = 7.60, ^{4}J = 1.20 Hz), 6.85 (ddd, 1H, H10, ^{3}J = 7.60, ^{3}J = 7.60, ^{4}J = 1.20 Hz). $^{13}C\{^{1}H\}$ NMR (DMSO-d6) δ = 163.0 (C6),159.3 (C1),153.3 (C7),147.1 (C5),144.8 (C8), 141.0 (C3), 132.8 (C11), 130.4 (C4),130.1 (C2), 129.4 (C12), 122.3 (C10),119.5 (C9).

2.6 Synthesis of complex [Ni(L^{2})Cl] (2c)

An equimolar mixture of 0.081 g (0.345 mmol) of $NiCl_2{\cdot}6H_2O$ in 25 mL of methanol with **2** (0.100 g, 0.345 mmol) was stirred at room temperature for 24 h. Then, the mixture obtained was filtered off and dried in vacuum. A dark red solid was formed and washed with diethylether, filtered off and dried by suction (3 x 15 mL). Deep red crystals were obtained by evaporation of a toluene-acetonitrile mixture (1:1). Yield: 69 % (0.091 g). M. p.: above 250 ^{o}C. Anal. Calc. for [$Ni(C_{18}H_{13}N_2S)Cl$] (%): 56.37% C, 3.42% H, 7.30% N. Found (%): 57.73% C, 3.07% H, 7.4% N. IR data (KBr, cm^{-1}): 1594, 1577 (C=N); 1588, 1471 (C=C).

3. Results and discussion

3.1 Synthesis of [M(L^n)Cl] complexes derived from 1–3.

Complexes of type [M(**L^n**)Cl] (M = Pd, Pt; n = 1–3) (**1a**–**3a** and **1b**–**3b**) were obtained from the equimolar reaction of the corresponding benzothiazoline **1–3** with the complex [M(NCMe)$_2$Cl$_2$] (M = Pd and Pt) in hot acetonitrile, whereas from the reaction of **3** with the nickel salt NiCl$_2$·6H$_2$O in hot methanol was obtained the complex [Ni(**L^3**)Cl] (**3c**), Scheme 2. The scheme numbering used herein after is also showed.

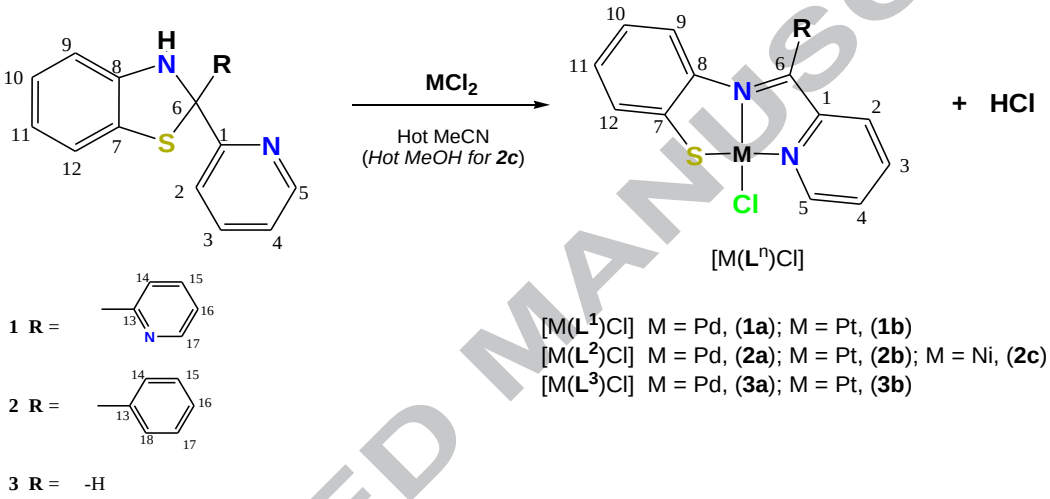

Scheme 2. Synthesis of [M(**L^n**)Cl] complexes of 10 Group containing ligand {**L^n**}$^-$. The numbering scheme for NMR data is showed.

The reaction of **1** with [Pd(NCMe)$_2$Cl$_2$] deserves a more detailed discussion. The green solid obtained was identified as a mixture of [Pd(**L^1**)Cl] and [Pd(**1**)Cl$_2$] in a 80:20 ratio by means of ^{1}H NMR spectroscopy. This mixture was heated at 60 °C for 5 min in dimethylsulfoxide, and the signals of [Pd(**1**)Cl$_2$] vanished. The ^{1}H NMR spectra just displayed signals attributable to [Pd(**L^1**)Cl] (**1a**). We also heated the mixture in acetonitrile; however, the ratio did not change. Moreover, our attempts to exclusively yield **1a** by means of the reaction of **1** with [Pd(NCMe)$_2$Cl$_2$] in hot dimethylsulfoxide resulted in a mixture of a large number of unidentifiable compounds.

Interestingly, when [Pd(NCMe)$_2$Cl$_2$] was added to **1** at 0 °C in acetonitrile and stirred for 24 h, the benzothiazoline displaced the solvent molecules and coordinated to Pd(II) to yield the complex [Pd(**1**)Cl$_2$] as a yellow solid (Scheme 3). This complex converts slowly to [Pd(**L**^{1})Cl] at room temperature, or quickly by heating it either in solution or in solid state. The formation of [Pd(**1**)Cl$_2$] as a complex of low stability at room temperature allow to appreciate the role of **1** as an effective ligand through of the coordination of two pyridinic substituents on the carbon atom of the thiazolidine ring, enhancing the formation of a *N,N*,-bidentate complex.

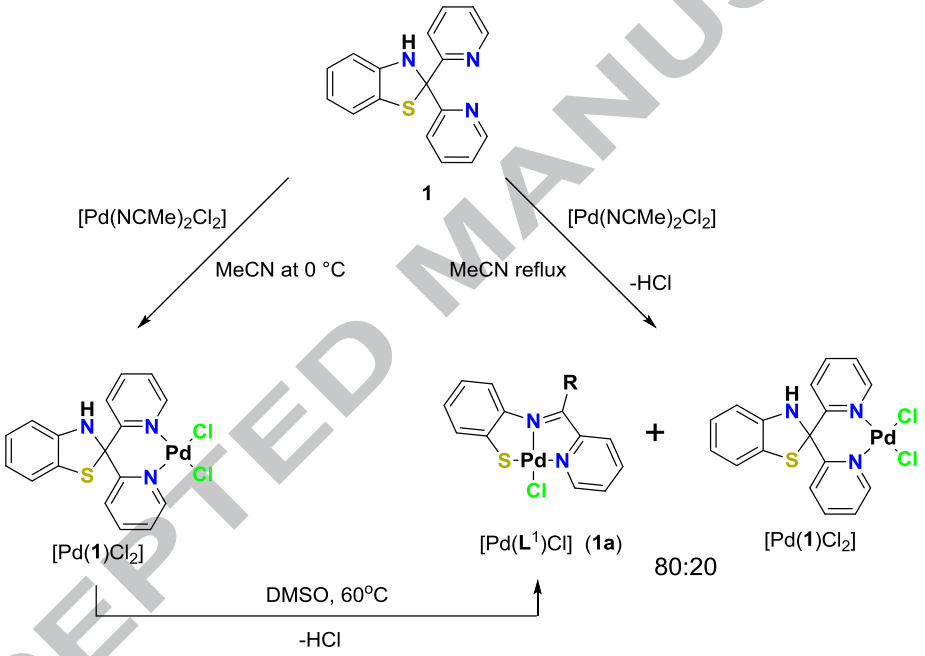

Scheme 3. Synthesis of Pd(II) complexes derived from **1** and **L**^{1}.

It is noteworthy that the benzothiazolines **2** and **3** with [M(NCMe)$_2$Cl$_2$] (M = Pd and Pt) at 0°C as well as compound **1** with the complex [Pt(NCMe)$_2$Cl$_2$] at low temperature did not react.

3.2. IR Spectroscopy

IR spectra of compounds **1**–**3** in CsCl showed the ν(NH) absorptions of the amino group in the 3340–3230 cm^{-1} range. The observation of the ν(NH) vibration agreed with the predominance of the benzothiazoline form in solid state; we did not observe bands assignable to H–S groups. For **1** and **2**, were observed single ν(NH) absorptions at 3287 and 3295 cm^{-1}, respectively. However, in the IR spectra of **3** were displayed two ν(NH) absorptions at 3340 (NH free) and 3230 cm^{-1} (NH hydrogen bond). The comparison of the ν(NH) absorptions for **1**–**3** at lower wavenumber respect to analogues containing free NH groups [[24], [25]] suggests the presence of hydrogen bonds of type NH---N. In order to establish the nature of the hydrogen bonds, the IR spectra of **1**–**3** in $CHCl_3$ were obtained. The ν(NH) absorption for **1** (3300 cm^{-1}), **2** (3337 cm^{-1}) and **3** (3288 cm^{-1}) in $CHCl_3$ solution was displayed at high wavenumber compared to the observed in CsCl (**1** at 3287, for **2** at 3295 and, for **3** at 3230 cm^{-1}). The frequencies observed in $CHCl_3$ solution were attributed to the prevalence of the NH---N intramolecular hydrogen bonds for **1**–**3**.

In the complex [Pd(**1**)Cl_2] the ν(NH) absorption at 3231 cm^{-1} is observed; for the complexes of type [M(**L**^{n})Cl] it is not observed. Respect to the ν(C=N) absorptions, for the complex [Pd(**1**)Cl_2] one absorption at 1600 cm^{-1} is indicative of a κ^2*N*-bidentate mode of **1**, while two absorptions in the range of 1605–1592 cm^{-1} and 1577–1534 cm^{-1} for the complexes [M(**L**^{n})Cl] (**1a**–**3a**, **1b**–**3b**, and **2c**) are indicative of κ^2*N*κ*S*-tridentate modes of the ligands {**L**^{n}}$^{-}$.

3.3. NMR Spectroscopy

^{1}H and ^{13}C{^{1}H} NMR spectra of benzothiazolines **1**–**3** as well as the spectra of [Pd(**1**)Cl_2] and [M(**L**^{n})Cl] (**1a**–**3a** and **1b**–**3b**) complexes were obtained at room temperature in DMSO-d6 solutions. The ^{1}H and ^{13}C{^{1}H} NMR spectra of the nickel compound **2c** displayed very broad signals. The numbering scheme utilized for NMR is shown in Scheme 2.

^{1}H and ^{13}C NMR spectra of **1**–**3** displayed the frequencies of the NH proton in the range of 7.84 to 7.12 ppm, whereas that the resonances for the C6 carbon are in

the 85.3–69.6 ppm range that has been associated with this type of quaternary carbon atoms in benzothiazoline derivatives [**Error! Bookmark not defined.**]. These data also support the benzothiazoline form as the predominant tautomer in solution, as we observed by IR spectra (*vide supra*).

On the other hand, the existence of hydrogen bonding interactions in DMSO-d6 solutions for benzothiazolines **1**–**3** was evaluated by means of the ^{1}H NMR shift dependence of the NH group with the temperature ($\Delta\delta/\Delta T$) [[26], [27]]. Thus, the $\Delta\delta/\Delta T$ values obtained from 363 to 295 K of -5.3×10^{-3}, -5.5×10^{-3}, and -4.4×10^{-3} ppm/K for **1**, **2**, and **3**, respectively, suggest the presence of intermolecular hydrogen bonding due to Me_2SO---HN interactions. We also analyzed the effect of the concentration of **1**, **2**, and **3** in a non-polar solvent such as $CDCl_3$ onto the chemical shift of the NH proton (1×10^{-1} and 1×10^{-3} M concentrations). ^{1}H NMR data for **1** and **2** displayed that these chemical shifts were independent of the concentration (6.75 ppm for **1**; 6.13 ppm for **2**, regardless the concentration), indicating the existence of NH---N intramolecular hydrogen bonding [[28]]. On the other hand, in compound **3** the NH proton was observed as a very broad resonance at 5.06 ppm in a 1×10^{-1} M solution, while for the more diluted solution, the NH resonance was not observed. The vanishing of this resonance at lower concentration suggests that this weak NH---N interaction is in fast exchange in $CDCl_3$ at room temperature.

In the ^{1}H NMR spectrum of [Pd(**1**)Cl_2] in DMSO-d6 solution, the NH proton at 8.82 ppm is displayed at higher frequencies in comparison with **1** (7.84 ppm); this deshielding is consistent with a reinforcement of the intermolecular hydrogen bond N–H---$OSMe_2$. We also observed two ABCD patterns for the pyridinic and phenyl protons, in a 2:1 ratio. In the complex [Pd(**1**)Cl_2] the magnetic equivalence of both pyridine rings is attributed to the coordination of **1** toward the palladium atom in a κ^2*N*-bidentate mode. In the case of [Pd(**L**^{1})Cl] both pyridine rings are not equivalents and the NH proton is missing; this observation agreed with a κ^2*N*κ*S*-tridentate mode of the deprotonated Schiff base {**L**^{1}}$^{-}$. Additionally, it is noteworthy that the pyridinic proton H5 in compounds **1**–**3** is observed in the 8.55 to 8.46 ppm range, whereas for the [Pd(**1**)Cl_2] and [M(**L**^{n})Cl] complexes the data range from

9.00 to 8.55 ppm; this shifting is attributed to the metallic bi- or tricoordination. In general, the metallic coordination in the complexes enhances the transformation of the ring forms of **1**-**3** into the open forms, i.e.; their Schiff bases, yielding the [M(**L^n**)Cl] complexes, where the NH proton has been lost.

The analysis of the $^{13}C\{^1H\}$ NMR data indicates that the chemical shift of the C6 carbon at 83.8 ppm agrees with a κ^2*N*-bidentate mode of **1** in the complex [Pd(**1**)Cl_2]; conversely, the frequencies of the carbon C6 in the range of 173.9 to 158.9 ppm indicate its iminic character, agreeing with a κ^2*N*κ*S*-tridentate coordination mode in the complexes [M(**L^n**)Cl] (**1a**–**3a** and **1b**–**3b**).

Table 1. Selected crystallographic data for **1**, **2**, **1a**–**3a**, **1b**·DMSO, and **2c**.

	1	**2**	**1a**	**2a**	**3a**	**1b**·DMSO	**2c**
Formula	$C_{34}H_{26}N_6S_2$	$C_{18}H_{14}N_2S$	$C_{17}H_{12}N_3SClPd$	$C_{18}H_{13}N_2SClPd$	$C_{24}H_{18}N_4S_2Cl_2Pd_2$	$C_{19}H_{18}N_3OS_2ClPt$	$C_{18}H_{13}N_2SClNi$
Formula weight	582.73	290.37	432.21	431.21	710.24	599.02	383.52
Crystal size (mm)	0.4 × 0.4 × 0.3	0.6 × 0.3 × 0.3	0.5 × 0.3 × 0.1	0.2 × 0.1 × 0.1	0.2 × 0.1 × 0.05	0.4 × 0.2 × 0.1	0.3 × 0.2 × 0.05
Crystal system	Triclinic	Orthorhombic	Monoclinic	Monoclinic	Triclinic	Monoclinic	Monoclinic
Space group	*P-1*	$P2_12_12_1$	$P2_1/n$	$P2_1/n$	*P-1*	$P2_1/c$	$P2_1/n$
a (Å)	8.0990(3)	9.9656(2)	10.3440(4)	12.1069(9)	7.0585(5)	12.5796(2)	12.1179(5)
b (Å)	11.3297(4)	10.4561(2)	10.9115(4)	7.1334(3)	10.6230(7)	19.2841(3)	7.1085(2)
c (Å)	15.9625(6)	13.9484(3)	14.9189(6)	19.2261(11)	17.4739(14)	8.27730(10)	18.8365(6)
α (°)	92.011(3)	90	90	90	85.169(6)	90	90
β (°)	90.204(3)	90	106.102(4)	104.946(7)	80.494(7)	99.607(2)	104.617(3)
γ (°)	91.716(3)	90	90	90	70.746(7)	90	90
V (Å^3)	1463.13(9)	1453.44(5)	1617.82(11)	1604.26(17)	1219.34(17)	1979.80(5)	1570.06(10)
Z	2	4	4	4	2	4	4
ρ_{calcd} (gm^{-3})	1.323	1.327	1.774	1.785	1.934	2.010	1.622
μ (mm^{-1})	1.921	1.911	1.442	12.064	15.694	16.592	4.571
F(000)	608.0	608.0	856.0	856.0	696.0	1152.0	784
GOF on F^2	1.028	0.982	1.068	1.015	1.161	1.057	1.036
T (K)	294	294	295	294	294	294	294
2θ range (°)	7.812 to 148.964	10.574 to 154.91	6.73 to 52.74	7.824 to 155.306	8.822 to 148.988	7.128 to 148.912	7.868 to 154.976
Reflections collected	24251	30691	27071	17138	10218	9715	16889
Unique reflections	5962	3090	3306	3373	4895	4054	3310
Absorption correction	multi-scan	multi-scan	multi-scan	multi-scan	multi-scan	multi-scan	multi-scan
Independent reflections (R_{int})	0.0279	0.0376	0.1326	0.0582	0.0716	0.0303	0.0502
R_1, wR_2 [I>2σ(I)]	0.0445, 0.1211	0.0358, 0.0950	0.0575, 0.1399	0.0422, 0.1009	0.0946, 0.2794	0.0303, 0.0774	0.0351, 0.0851
R_1, wR_2 [all data]	0.0551, 0.1327	0.0392, 0.0991	0.0727, 0.1607	0.0690, 0.1194	0.1169, 0.2890	0.0333, 0.0807	0.0506, 0.0948
Largest residuals (eÅ^{-3})	0.38/−0.32	0.31/−0.23	1.92/−1.62	1.12/−0.58	2.62/−0.98	1.35/−0.85	0.33/−0.23
Flack parameter	-	0.001(6)					

Table 2. Selected bond lengths [Å] and angles [°] for **1**, **2**, **1a**–**3a**, **1b**·DMSO, and **2c**.

Compound	**1**		**2**	**1a**	**2a**	**3a**		**1b**·DMSO	**2c**
M	**-**		**-**	**Pd**	**Pd**	**Pd**		**Pt**	**Ni**
	Molecule 1	*Molecule 2*				*Molecule 1*	*Molecule 2*		
C(1)–N(1)	1.331(3)	1.313(3)	1.334(4)	1.365(7)	1.357(6)	1.35(2)	1.34(2)	1.376(5)	1.358(3)
C(6)–C(1)	1.529(3)	1.532(3)	1.526(4)	1.477(7)	1.489(7)	1.50(3)	1.49(3)	1.477(5)	1.469(3)
C(6)–N(2)	1.457(2)	1.456(2)	1.464(3)	1.295(6)	1.287(7)	1.24(2)	1.25(2)	1.309(5)	1.294(3)
C(6)–S(1)	1.8525(19)	1.8543(19)	1.869(2)	---	---	---		---	---
C(7)–S(1)	1.765(2)	1.765(2)	1.755(3)	1.758(6)	1.766(7)	1.757(16)	1.750(18)	1.755(4)	1.748(3)
C(8)–N(2)	1.389(3)	1.392(3)	1.384(3)	1.425(6)	1.434(7)	1.43(2)	1.41(2)	1.426(5)	1.430(3)
N(1)–M				2.050(5)	2.053(5)	2.082(14)	2.082(16)	2.036(3)	1.935(2)
N(2)–M				2.013(4)	2.001(4)	2.012(13)	1.998(13)	1.980(3)	1.8849(17)
M–S(1)				2.2301(16)	2.2369(19)	2.255(5)	2.252(5)	2.2545(11)	2.1501(8)
M–Cl(1)				2.2974(15)	2.2949(14)	2.283(5)	2.281(5)	2.3039(11)	2.1701(7)
C(1)–C(6)–N(1)				115.6(4)	114.7(5)	114.3(16)	117.5(18)	116.3(3)	113.5(2)
C(8)–N(2)–C(6)				129.5(4)	128.1(4)	127.7(16)	125.1(16)	127.5(3)	126.28(19)
C(7)–S(1)–M				96.01(18)	96.5(2)	96.7(6)	96.4(6)	96.15(13)	97.59(8)
N(2)–C(6)–S(1)	102.74(13)	102.54(13)	104.09(16)	-----	-----	-----	-----	-----	-----
C(8)–N(2)–C(6)	112.81(15)	111.50(15)	115.1(2)	-----	-----	-----	-----	-----	-----
C(7)–S(1)–C(6)	90.72(9)	89.50(9)	91.96(12)	-----	-----	-----	-----	-----	-----
N(1) –M–N(2)				81.66(16)	81.19(17)	80.6(6)	81.0(6)	81.28(13)	83.87(8)
N(1) –M–S(1)				168.57(13)	169.36(12)	168.2(5)	168.3(4)	168.87(9)	172.88(6)
N(1)–M–Cl(1)				96.97(13)	96.68(13)	97.3(5)	97.4(5)	96.93(9)	96.27(6)

3.4 X-ray crystallographic studies

Crystalline structures in solid state of **1**, **2**, **1a**–**3a**, **1b**, and **2c** were stablished by single-crystal X-ray diffraction analyses at room temperature. The complex **1b** was crystallized as a DMSO solvate. Crystallographic data are summarized in Table 1 and selected bond distances and angles are shown in Table 2. X-ray analyses of **1** and **3a** displayed two independent molecules in the asymmetric unit.

3.4.1 Molecular and crystalline structures of 1 and 2.

The molecular structures for compounds **1** and **2** are showed in Figure 2. The analyses revealed that the bond lengths around the tetrahedral quaternary carbon C(6) agree with the benzothiazoline form as the predominant one in solid state, and are similar to other analogues where the substituents at C(6) atom are hydrogen and phenyl groups [**Error! Bookmark not defined.**]. In this pair of compounds there are several noncovalent interactions in the crystalline state mainly due to the presence of hydrogen atoms covalently linked to electronegative nitrogen atoms, besides to the presence of CH---S interactions and aromatic rings. To describe the intermolecular interactions based on hydrogen bonding, we used the graph analysis approach [[29]]. Both compounds exhibit intramolecular NH---N and CH---S hydrogen bonds, and are described at the first level as $S_1^1(5)$. The first one is formed between the NH of the thiazoline ring and the pyridinic nitrogen atom of one molecule, while the second intramolecular CH---S interaction is displayed between the sulfur atom of the heterocyclic ring and the H2 of the pyridinic ring. Both crystallographic different molecules in **1** also display centrosymmetric dimers linked by intermolecular hydrogen bonds between the NH of thiazolidine ring of one molecule and the pyridinic nitrogen of a neighboring molecule (Figure 3), described by $R_2^2(10)$. For **2**, interactions of type CH$\cdots\pi$ [2.684 Å; interplanar angle 77.03°] were observed; the molecules are related by a binary screw axis along the b direction (Figure 3).

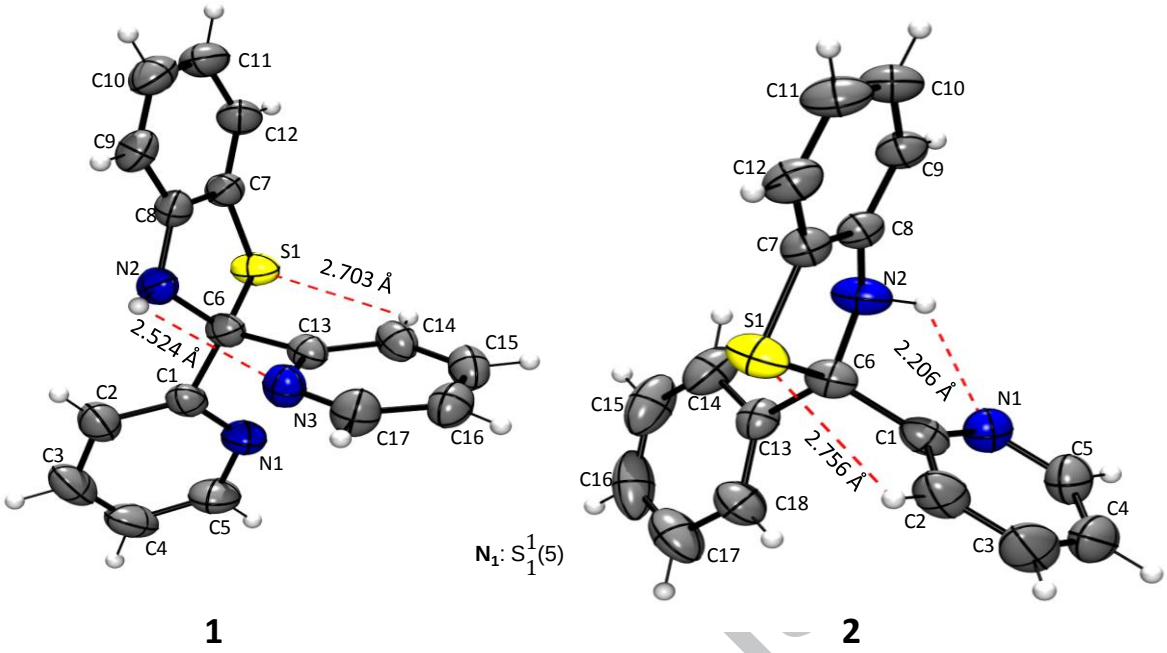

Figure 2. Molecular drawing of benzothiazolines **1** and **2** (ORTEP 50% probability).

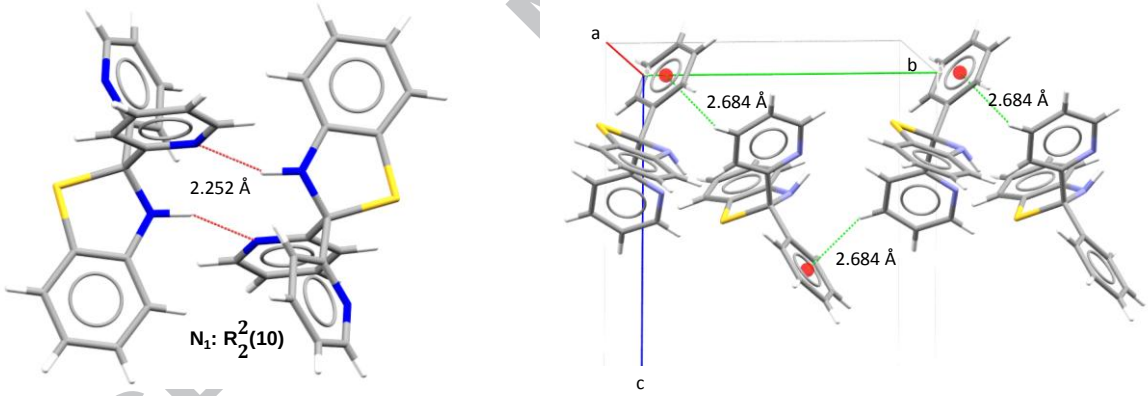

Figure 3. Hydrogen bonding and CH···π interactions in **1** and **2**.

3.4.2 Molecular and crystalline structures of complexes [M(L^n)Cl]

Structures of compounds of general formula [M(**L**^{n})Cl] consist of neutral mononuclear complexes with a distorted square planar local geometry for the M(II) central cation, where the benzothiazoline compounds have been transformed to their corresponding Schiff bases, i.e., into their deprotonated open form {**L**^{n}}$^-$

(Figure 4). In all complexes, the Schiff bases displayed a κ^2*N*,κ*S*- tridentate coordination mode, forming two five-membered chelate rings in a planar conformation. The M-N(2) bond lengths of the iminic nitrogen atom in all complexes are shorter than the M-N(1) lengths involving the pyridinic nitrogen atom. These lengths are similar to those previously described for nickel, palladium, and platinum complexes, [[30], [31], [32], [33], [34]], and they are indicative that the iminic coordination compared to the pyridinic one is stronger, figure 5 [[35]]. In particular, for the isostructural complexes **1a** and **1b**, the close similitude of the bond distances around the metallic center (Pd or Pt) can be attributed to the lanthanide contraction effect present in the 5d platinum(II) cation.

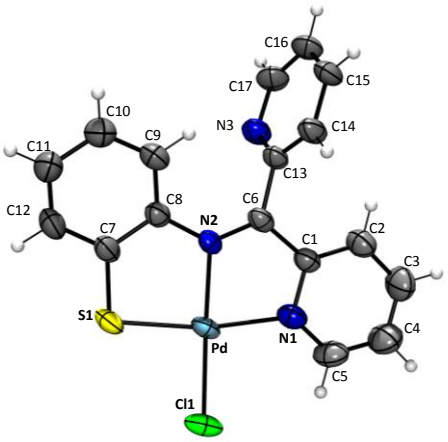

[Pd(**L**^{1})Cl] (**1a**)

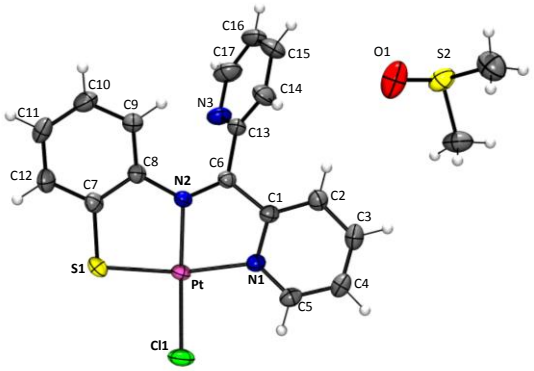

[Pt(**L**^{1})Cl]•DMSO (**1b**•DMSO)

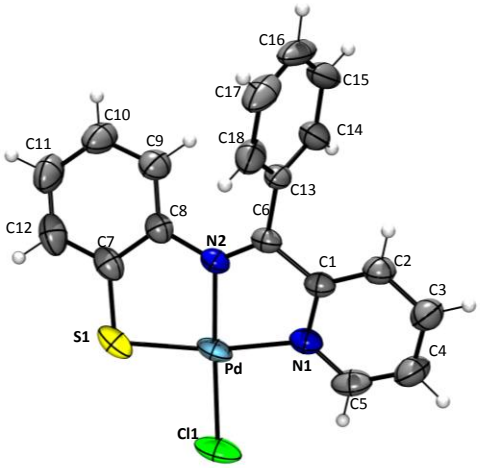

[Pd(**L**^{2})Cl] (**2a**)

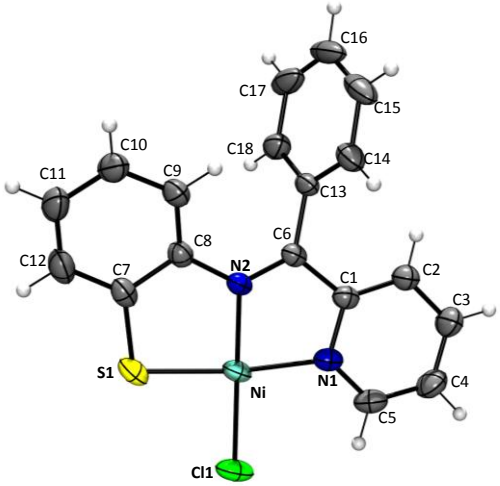

[Ni(**L**^{2})Cl] (**2c**)

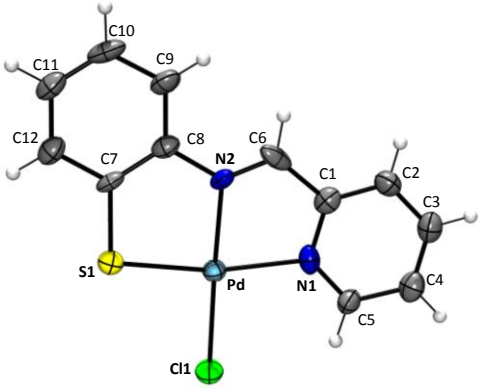

[Pd(**L**^{3})Cl] (**3a**)

Figure 4. Molecular structures of complexes [M(**L**^{n})Cl] (ORTEP 50% probability).

In the crystals of **1a**, **2a**, **1b**·DMSO, and **2c** were observed dimeric centrosymmetric M---M interactions in a head-to-tail fashion [**1a**, 3.5969(7) Å; **2a**, 3.6232(8) Å; **1b**·DMSO of 3.6218(3) Å; **2c**, 3.634(8) Å]. These M---M interactions are larger than the van der Waals radii sum [Σr_{vdW}(Pd, Pd) = 3.26 Å; (Pt, Pt) = 3.44 Å] [[36]]; we adopted a less restricted criteria to analyze the intermolecular interactions (ca. 4.0 Å) in conjunction with geometrical features. The M---M interactions observed in our complexes are comparable to those observed in square planar Ni(II), Pd(II), and Pt(II) complexes containing in their coordination entity one chloro and either *N,N,S*- or *S,S,N*-tridentate ligands; the Pd---Pd lengths in the complexes **1a** and **2a** are longer than the interactions described for analogues of Pd(II) [36, [37]], whilst in **1b** the Pt---Pt length is shorter than the interaction found in the analogue complex of Pt(II) [[38]].

The compounds derived from the benzothiazoline **1** displayed both centrosymmetric arrangements between two molecules linked by weak hydrogen bonding (Figure 5).

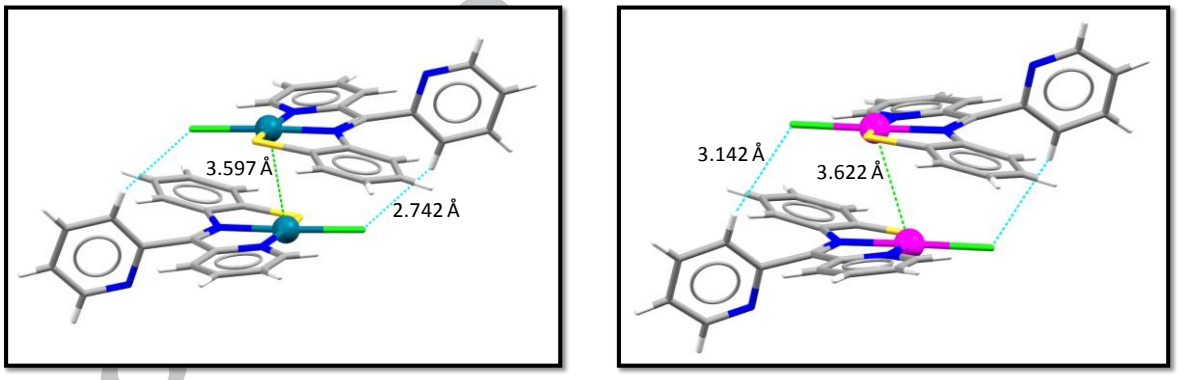

[Pd(**L**^{1})Cl] (**1a**) [Pt(**L**^{1})Cl]·DMSO (**1b** ·DMSO)

Figure 5. Centrosymmetric dimers of **1a** and **1b**·DMSO (the molecule of DMSO has been omitted)

On the other hand, the structures of the palladium and nickel complexes **2a** and **2c** are isomorphic (both crystallized in the $P2_1/n$ space group); the cell parameters are shorter in the case of the smaller Ni(II) cation. Both displayed a similar arrangement in the crystal, with CH---Cl and M---S (not showed for clarity)

interactions; in the figure 6 is showed the arrangement for the Ni(II) complex, where the figures in parentheses are for the Pd(II) complex (**2a**). The difference of **2a** and **2c** with the compounds containing a pyridinic substituent (**1a** and **1b**·DMSO) is the presence of two CH---Cl interactions, because of the unsubstituted phenyl group attached to C6.

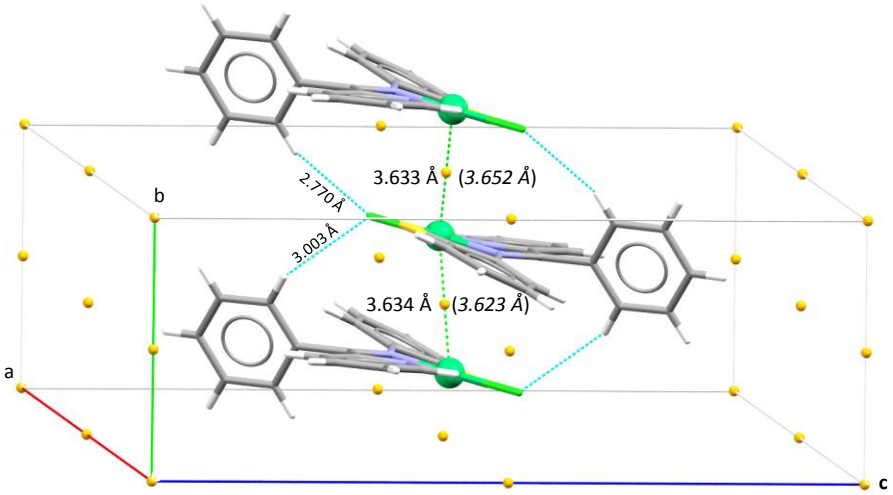

Figure 6. Crystal packing of [Ni($\mathbf{L}^2$)Cl] (**2c**) showing some intermolecular interactions (Ni---S, 3.353 Å; Pd---S, 3.605 Å). The data in parenthesis are for the isomorphic compound **2a**; yellow circles represent the inversion centers in the $P2_1/n$ space group.

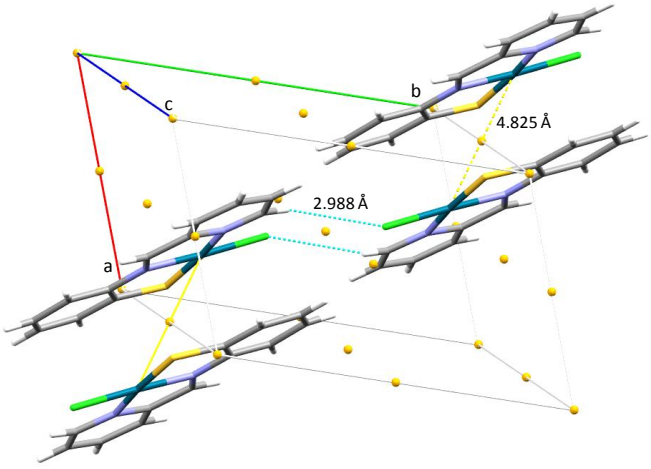

Figure 7. Crystal packing of [Pd($\mathbf{L}^3$)Cl] (**3a**) showing CH---Cl interactions; yellow circles represent the inversion centers in the *P−1* space group.

3.5. DFT studies

Several authors have mentioned the possible equilibrium between the ring (or closed) form and the open (Schiff base) form. We study this equilibrium by DFT methods. The proposed tautomerization mechanisms of benzothiazolines **1**–**3** are shown in Figure 8 along their calculated energy profiles. Free energy changes ΔG, activation barriers $\Delta G^{\dagger}$ and equilibrium constants K_{eq} of the ring-open form conversions of compounds **1** (**1**→H**L**^{1}), **2** (**2**→H**L**^{2}) and **3** (**3**→H**L**^{3}) are reported in Table 3. The small values of the calculated equilibrium constants reveal that the equilibria are strongly shifted towards the ring forms. These values agree with the experimental data obtained in solution and solid state, which supports the ring form (benzothiazoline) as the predominant tautomer for **1**–**3**.

Table 3. Free energy changes ΔG, activation barriers $\Delta G^{\dagger}$, and equilibrium constants Keq for the tautomerization of **n**→H**L**^{n} (n = **1**, **2**, **3**) and for the formation of complexes **1a**–**3a**, calculated in gas phase at 273 K at the PBEPBE/(Def2-TZVP,SDD) level of theory.

Reaction	$\Delta G^{\dagger}$/kcalmol^{-1}	ΔG/kcalmol^{-1}	K_{eq}
1→H**L**^{1}	30.7	10.4	4.53×10^{-9}
2→H**L**^{2}	27.0	4.7	1.89×10^{-4}
3→H**L**^{3}	32.1	7.2	1.65×10^{-6}
1→**1a** (pathway A)	22.8	−18.0	2.5×10^{14}
1→**1a** (pathway B)	21.7	−18.0	2.5×10^{14}
2→**2a**	23.4	−21.5	1.5×10^{17}
3→**3a**	24.2	−22.0	4.0×10^{17}
[Pd(**1**)Cl_2]→**1**	31.9	10.2	6.9×10^{-9}
[Pd(**1**)Cl_2]→**1a**	23.0	−7.8	1.7×10^{6}

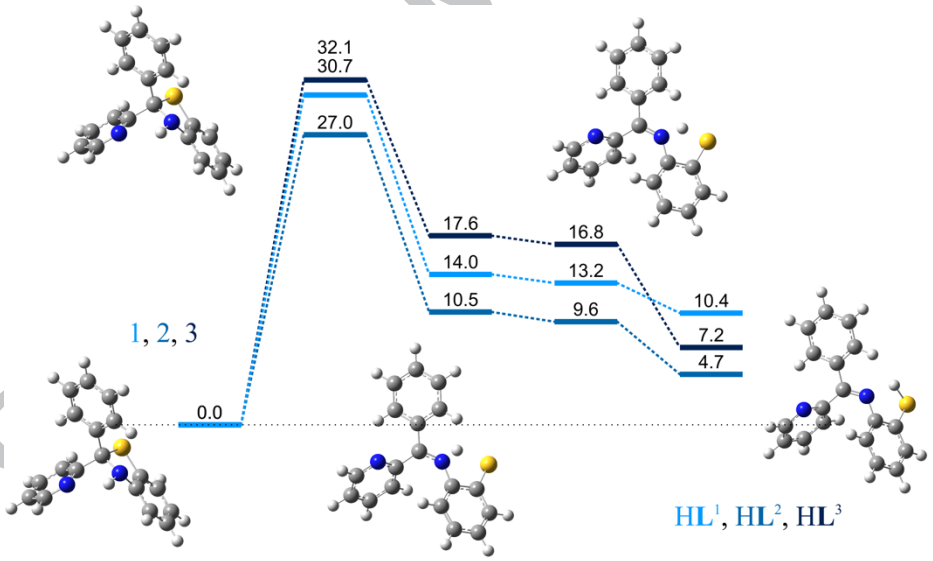

Figure 8. Free energy profile relative to the benzothiazolines **1**–**3** (reactants) (kcalmol^{-1}) for their tautomerization process to yield Schiff bases H**L**^{1} (light blue) H**L**^{2} (blue), and H**L**^{3} (dark blue), calculated in gas phase at 273 K at the PBEPBE/(Def2-TZVP,SDD) level of theory. (Molecular structures correspond to the tautomerization of **1** to H**L**^{1}).

We also studied the formation of complexes of palladium **1a**–**3a**. In this case, two different reaction pathways are proposed (Figure 9). Mechanisms A (shown in blue) are common to the three complexes **1a–3a** and only differ in their relative energies due to the different R groups. On the other hand, mechanism B (shown in green) is exclusive to compound **1a**. Mechanism B proceeds through the *N,N*-bidentate complex [Pd(**1**)Cl_2] and matches with mechanism A just before the final step. It is noteworthy that this intermediate is highly stable (10.2 $kcalmol^{-1}$ more stable than the reactants) with backward and forward activation barriers of 31.9 and 23.0 $kcalmol^{-1}$, respectively, as shown in Table 3. Therefore, once [Pd(**1**)Cl_2] is formed, the backward reaction is unlikely because the large activation barrier, while the forward reaction will proceed easily at room temperature. On the other hand, activation barriers at 0 ºC of mechanisms A and B are 22.8 and 21.7 $kcalmol^{-1}$ respectively, indicating that mechanism B will be preferred at this temperature. This result agrees with the observation of [Pd(**1**)Cl_2] in solution by NMR. Moreover, the very large equilibrium constants of the complexation reactions demonstrate that they are irreversible.

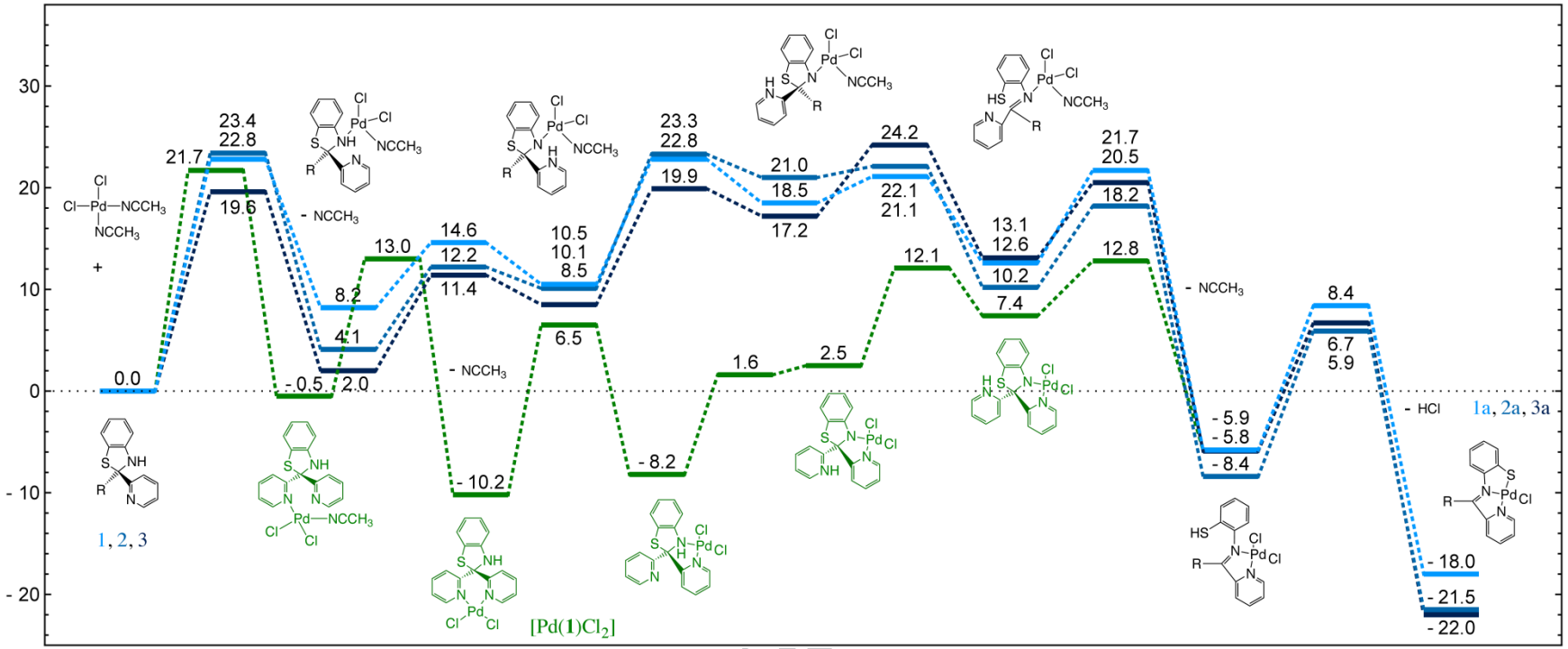

Figure 9. Free energy profiles relative to the **1–3** reactants (kcalmol^{-1}) for the formation of palladium(II) compounds **1a** (red and light blue), **2a** (blue) and **3a** (dark blue) calculated in gas phase at 273 K at the PBEPBE/(Def2-TZVP,SDD) level of theory. Two different mechanisms, A (blue) and B (green) are possible for compound **1a**.

Conclusions

Benzothiazolines **1**–**3** towards 10 Group metals at higher temperatures displayed the opening of the thiazoline ring with the observation of anionic Schiff bases $\{\mathbf{L^n}\}^-$ coordinated to Ni(II), Pd(II), and Pt(II). The $\{\mathbf{L^n}\}^-$ exhibited a *N,N,S*-tridentate coordination mode forming two five-membered chelate rings. In all complexes was displayed a local geometry distorted square planar around the metal ions.

The benzothiazolines **1**–**3** in presence of Ni(II), Pd(II), and Pt(II) ions displayed significant differences in reactivity that are attributed to the R substituent linked to the carbon atom C6 of the thiazoline heterocyclic. In particular, the presence of two pyridinic substituents in **1** enhances the formation of the coordination complex [Pd(**1**)Cl_2] at low temperature. In this complex, it is observed a six-membered chelate ring, where **1** exhibit a *N,N*-bidentate coordination mode. Moreover, our DFT studies indicated the role of [Pd(**1**)Cl_2] as a key chemical species in the formation of the compound having the Schiff base $\{\mathbf{L^1}\}^-$ as a ligand. On the other hand, for **2** and **3** the reaction pathways are consistent with the formation of $N_{thiazoline}$-coordinated intermediates for the ring opening transformations.

Supplementary data

Supplementary data are available from the Cambridge Crystallographic Data Centre with the deposition numbers CCDC 1554005 (**1**), 1554007 (**2**), 1554004 (**1a**), 1554006 (**2a**), 1554003 (**3a**), 1554002 (**1b**·DMSO), 1554008 (**2c**). These data can be obtained free of charge *via* http://www.ccdc.cam.ac.uk (or from the Cambridge Structural Data Centre, 12 Union Road, Cambridge, CB2 1EZ, UK; Fax: +44 1223 336033).

Acknowledgements

JAAH fully acknowledges the scholarship from CONACYT. This research was partially supported by projects “Integración de Redes Temáticas de Colaboración Académica 2015 SEP” and “ABACUS, CONACYT-EDOMEX-2011-C01-165873” for the computing facilities.

References

References

[1] Ch. Zhu, T. Akimaya, *Tetrahedron Lett.* **53** (2012) 416-418.

[2] C. Zhu, K. Saito, M. Yamanaka, T. Akiyama, *Acc. Chem. Res.* **48** (2015) 388−398

[3] M. A. Lynn, L. J. Carlson, H. Hwangbo, J. M. Tanski, L. A. Tyler, *J. Mol. Struct.***1011** (2012) 81-93

[4] S. Mitra, A. Chakrabrorty, S. Mishra, A. Majee, A. Hajra, *Org. Lett.* **16** (2014), 5652-5655.

[5] S. Metz, C. Burschka, R. Tacke, *Eur. J. Inorg. Chem,* (**2008),** 4433–4439

[6] F. Fülöp, J Mattinen, K. Pihlaja, *Tetrahedron* **46** (1990) 6545–6552.

[7] F. Fülöp, L. Lázar, G. Bernáth, I. Pelczer, *Tetrahedron* **44** (1988) 2993-2996.

[8] M. M. H. Khalil, F. A. Al-Seif, *J. Saudi Chem. Soc.***14** (2010) 33-39.

[9] K. M. Chauhan, S. C. Joshi, *Inorg. Lett.* **1** (2014) 23-35

[10] L. J. Carlson, J. Welby, K. A. Zebrosky, M. M. Wilk, R. Giroux, N. Ciancio, J. M. Tanski, A. Bradley, L. A. Tyler, *Inorg. Chim. Acta* **365** (2011) 159-166.

[11] J. R. Anacona, V. E. Marquez, Y. Jimenez, *J. Coord. Chem.* **62** (2009) 1172–1179.

[12] U. K. Das, S. L. Daifuku, S. I. Gorelsky, I. Korobkov, M. L. Neidig, *Inorg. Chem.* (2016) 987-997.

[13] S. Sharma, R. K. Sharma, A. K. Rai, Yashpal Singh, *Heteroatom Chem*. **15** (2004) 92-96.

[14] R. Contreras, H. R. Morales, Ma. de L. Mendoza, C. Domínguez. *Spectrochim. Acta.* **43** (1987) 43-49.

[15] C. J. Mathews, P. J. Smith, T. Welton, J. *Mol. Catal. A. Chem.* **206** (2003) 77-82.

[16] Oxford Diffraction CrysAlis software system, version 1.171.37.35. Oxford Diffraction Ltd., Abingdon, UK (2014).

[17] SHELXTL 6.14 Bruker AXS, Inc. Madison. WI. USA, (2006).

[18] O.V. Dolomanov, L.J. Bourhis, R.J. Gildea, J.A.K. Howard, H. Puschmann, *J. Appl. Cryst.* **42** (2009) 339-341.

[19] NIST Webbook at http://webbook.nist.gov/cgi/cbook.cgi?Name=acetonitrile

[20] Open Cristallographic database at http://www.crystallography.net/cod/cod/1010447.html

[21] B. Aradi, B. Hourahine, T. Frauenheim, *J. Phys. Chem.* **111** (2007) 5678-5684.

[22] M. J. Frisch, G. W. Trucks, H. B. Schlegel, G. E. Scuseria, M. A. Robb, J. R. Cheeseman, G. Scalmani, V. Barone, B. Mennucci, G. A. Petersson, H. Nakatsuji, M. Caricato, X. Li, H. P. Hratchian, A. F. Izmaylov, J. Bloino, G. Zheng, J. L. Sonnenberg, M. Hada, M. Ehara, K. Toyota, R. Fukuda, J. Hasegawa, M. Ishida, T. Nakajima, Y. Honda, O. Kitao, H. Nakai, T. Vreven, J. A. Montgomery Jr., J. E. Peralta, F. Ogliaro, M. Bearpark, J. J. Heyd, E. Brothers, K. N. Kudin, V. N. Staroverov, R. Kobayashi, J.

Normand, K. Raghavachari, A. Rendell, J. C. Burant, S. S. Iyengar, J. Tomasi, M. Cossi, N. Rega, N. J. Millam, M. Klene, J. E. Knox, J. B. Cross, V. Bakken, C. Adamo, J. Jaramillo, R. Gomperts, R. E. Stratmann, O. Yazyev, A. J. Austin, R. Cammi, C. Pomelli, J. W. Ochterski, R. L. Martin, K. Morokuma, V. G. Zakrzewski, G. A. Voth, P. Salvador, J. J. Dannenberg, S. Dapprich, A. D. Daniels, O. Farkas, J. B. Foresman, J. V. Ortiz, J. Cioslowski, D. J. Fox, Gaussian-09, Revision A.1, Gaussian Inc., Wallingford, CT, 2009.

[23] G. Geudtner, P. Calaminici, J. Carmona-Espíndola, J. del Campo, V. D. Domínguez-Soria, R. Flores-Moreno, G. U. Gamboa, A. Goursot, A. M. Köster, J. U. Reveles, T. Mineva, J. M. Vásquez-Pérez, A. Vela, B. Zuñinga-Gutierrez, D. R. Salahub, *WIREs: Comput. Mol. Sci.* **2** (2012) 548-555.

[24] H. Böhlig, M. Ackermann, F. Billes, M. Kudra, M. Kudra *Spectrochim. Acta*, Part A 55 (1999) 2635-2646.

[25] J. Kuwabara, H. Mori, T. Kanbara, *Heterocycles* **78** (2009) 2605-2607.

[26] S. H. Gellman, B. R. Adams, G. P. Dado, *J. Am. Chem. Soc.* **112** (1990) 460-461.

[27] S. G. Gellman, G. P. Dado, G. Liang, B. R. Adams, *J. Am. Chem. Soc.* **113** (1991) 1164-1173.

[28] J. A. Raymond, M. Mehdi, *Magn. Reson. Chem.* **45** (2007) 865-877

[29] J. Bernstein, R. E. Davis, L. Shimoni, N.-L. Chang, *Angew. Chem. Int. Ed. Engl.* **34** (1995) 1555-1573

[30] N. H. Hung, L. D. Canh, P. T. Chien, T. N. Thi, H. Adelheid, A. Ulrich, *Polyhedron* **48** (2012) 181-188.

[31] D. Kovala-Demertzi, M. A. Demertzis, Alfonso Castiñeiras, D. X. West, *Polyhedron* **17** (1998) 3739-3745.

[32] K. I. Goldberg, J. Valdes-Martınez, G. Espinosa-Perez, L. J. Ackerman, D. X. West, *Polyhedron* **18** (1999) 1177-1182.

[33] F. Teixidor, P. Anglès, C. Viñas, R. Kivekä, R. Sillanpää, *Inorg. Chem.* **38** (1999) 1642-1644.

[34] D. Kovala-Demertzi, P. N. Yadav, M. A. Demertzis, M, Coluccia, *J. Inorg. Biochem.* **78** (2000) 347-354.

[35] D. Kovala-Demertzi, M. Demertzis, P. N. Yadav, A. Castiñeiras, D. X. West, *Transition Met. Chem.*, **24** (1999) 642-647.

[36] W.W. Porterfield, Inorganic Chemistry: A Unified Approach, second ed., Academic Press Inc., USA, 1993. p. 214.

[37] V. Muthalagu, L. Yee-Hing, M. K. Fun, *Inorg. Chim. Acta* **357** (2004) 1397-1404

[38] D. Kovala-Demertzia, M. A. Demertzisa, J. R. Millera, C. Papadopoulou, C. Dodorou, G. Filousis, *J. Inorg. Biochem.* **86** (2001) 555-563.

Graphical Abstract Synopsis

Three pyridylbenzothiazolines of general formula [(C_6H_4NCS)(C_5H_4N)R] (R = C_5H_4N, **1**; R = C_6H_5, **2**; R = H, **3**) with chlorides of Ni(II), Pd(II), and Pt(II) were used as precursors for the formation of metallic complexes of the Schiff bases. The opening reactions of the thiazoline ring gave tricoordinate metallic complexes of type [M(**L**^{n})Cl]. Crystals structures of complexes **1a**–**3a**, **1b**·DMSO, and **2c** are stabilized by M**---**M, π···π, or CH---Cl interactions. The predominance of the benzothiazoline (ring form) and the formation of complexes [Pd(**L**^{n})Cl] (*n* = 1-3) by DFT calculations were evaluated.